Role of the reaction intermediates in determining PHIP (parahydrogen induced polarization) effect in the hydrogenation of acetylene dicarboxylic acid with the complex [Rh (dppb)]+ (dppb: 1,4-bis(diphenylphosphino)butane)

F. Reineri, S. Aime, R. Gobetto, and C. Nervi

Citation: The Journal of Chemical Physics **140**, 094307 (2014); doi: 10.1063/1.4867269
View online: http://dx.doi.org/10.1063/1.4867269
View Table of Contents: http://scitation.aip.org/content/aip/journal/jcp/140/9?ver=pdfcov
Published by the AIP Publishing

Role of the reaction intermediates in determining PHIP (parahydrogen induced polarization) effect in the hydrogenation of acetylene dicarboxylic acid with the complex [Rh (dppb)]$^+$ (dppb: 1,4-bis(diphenylphosphino)butane)

F. Reineri,[1] S. Aime,[1] R. Gobetto,[2] and C. Nervi[2]
[1]*Department of Molecular Biotechnologies and Health Sciences, University of Torino, Via Nizza 52, 10123 Torino, Italy*
[2]*Department of Chemistry, University of Torino, via P. Giuria 7, 10125 Torino, Italy*

(Received 9 October 2013; accepted 18 February 2014; published online 7 March 2014)

This study deals with the parahydrogenation of the symmetric substrate acetylene dicarboxylic acid catalyzed by a Rh(I) complex bearing the chelating diphosphine dppb (1,4-bis(diphenylphosphino)butane). The two magnetically equivalent protons of the product yield a hyperpolarized emission signal in the ^{1}H-NMR spectrum. Their polarization intensity varies upon changing the reaction solvent from methanol to acetone. A detailed analysis of the hydrogenation pathway is carried out by means of density functional theory calculations to assess the structure of hydrogenation intermediates and their stability in the two solvents. The observed polarization effects have been accounted on the basis of the obtained structures. Insights into the lifetime of a short-lived reaction intermediate are also obtained. © *2014 AIP Publishing LLC*. [http://dx.doi.org/10.1063/1.4867269]

I. INTRODUCTION

The hydrogenation mechanism of unsaturated substrates using cationic Rh(I) complexes has been extensively investigated by means of kinetic studies,[1] density functional theory (DFT) calculations,[2–4] and, more recently, ParaHydrogen Induced Polarization (PHIP).[5–7] The interest in this class of catalysts, in particular with chelating phosphine, namely [(P-P)Rh(I)(diene)], for parahydrogenation reactions is due to the high polarization level that can be achieved on both ^{1}H and heteronuclear signals. In the presence of these Rh(I) complexes, the hydrogenation reaction follows the so-called unsaturated route (Figure 1),[1] in which the substrate is coordinated to the metal first and then hydrogen is irreversibly transferred to the unsaturated molecule. This behavior makes the Rh(I) complexes containing a chelating phosphine more suitable for the attainment of a high polarization level on the hydrogenated products than other Rh compounds such as Wilkinson catalyst.[9] It was also found that singlet-triplet mixing can occur on reaction intermediates and this can be exploited to gain mechanistic information about intermediate hydrogen complexes and an estimate of the dwell time of the hydrogen nuclei in magnetically inequivalent positions.[8]

Transient dyhidride intermediates are extremely elusive and they have never been observed, except in one case, using parahydrogen with an unusually reactive complex at low temperature.[10] Nevertheless, hyperpolarization attained on products is often much lower than that theoretically predicted,[5] even with this kind of catalyst.

In this work it is shown how the level of polarization obtained on the hydrogenated product is also influenced by the structure and lifetime of these reaction intermediates, in fact an intermediates stability change due to the interaction with different solvent molecules leads to different hyperpolarization level. In particular the parahydrogenation reaction of acetylenedicarboxylic acid (ADC) catalyzed by [Rh(COD)(dppb)][BF_4] (COD = cyclooctadiene, dppb = diphenylphosphinobutane) is studied, on which the two protons are added to magnetically equivalent positions.

Symmetrical substrates have already been shown to yield ^{1}H polarized patterns due to reaction intermediates[11] or to long range coupling with other protons of the product.[12]

DFT optimization of the reaction intermediates and transition states are carried out in order to obtain mechanistic support to the experimentally observed PHIP effects and, in turn, to elucidate the occurring hydrogenation pathway. These calculations provide a direct access to structure and stability of intermediates, which are responsible for the observed polarization effects.

II. EXPERIMENTAL METHODS

A. Parahydrogenation experiments

Parahydrogenation reactions are carried out in acetone or methanol using the commercial catalyst [Rh(COD)(dppb)][BF_4] (COD = cyclooctadiene, dppb = diphenyl-phosphinobutane). This catalyst is purchased from Aldrich and used without further purification.

The ^{13}C enriched substrate 1-^{13}C ADC has been synthesized as previously reported.[13]

To carry out the ALTADENA experiments,[5] NMR tubes equipped with Young valves are charged with a 3–4 mM solution of the catalyst. Before substrate addition, the catalyst is activated by hydrogenation of the coordinated diene COD to yield the active form [Rh(dppb)S_2]$^+$, where S = solvent.

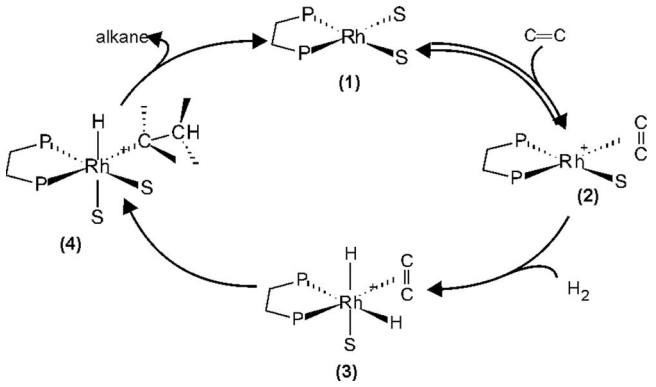

FIG. 1. Hydrogenation catalytic cycle called "unsaturated route." S = solvent.

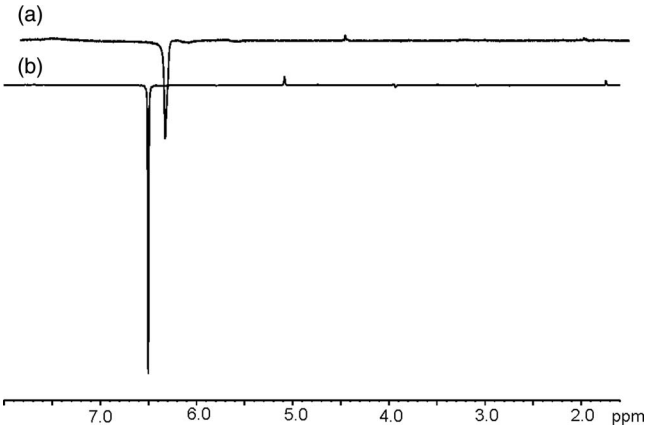

FIG. 2. ^{1}H-NMR polarized olefinic signal of maleic acid obtained from parahydrogenation of ADC in methanol (b) and in acetone (a). ALTADENA experiment, 10 bars parahydrogen in the gas-tight NMR tube.

Then the substrate ADC is added (35 mM), the solution degassed by freeze-thaw-pump cycle and pressurized with 10 bars of parahydrogen (50% para enriched). The solution is heated to room temperature in about 30", then the parahydrogenation reaction is started by means of vigorous shaking of the NMR tube at low magnetic field (earth field). ^{1}H and ^{13}C-NMR spectra are acquired on Bruker Advance 600 spectrometer.

Parahydrogenation experiments in PASADENA[5] conditions are carried out by bubbling p-H_2 (1 bar) through the hydrogenation mixture into the NMR spectrometer for 10 s. In this case the catalyst concentration is 15 mM. In order to be able to compare the intensity of polarized ^{1}H emission signal with that achieved in the ALTADENA experiment, parahydrogenation is also carried out by flowing parahydrogen at atmospheric pressure into the hydrogenation mixture at low magnetic field. Then the sample is placed into the spectrometer in about 5 s and the ^{1}H-NMR spectrum is acquired. In both cases, ALTADENA and PASADENA experiments, the spectrum is acquired by applying a 90° pulse.

B. Computational

All calculations are performed with the Gaussian 09 (G09) program package employing the DFT method with Becke's three parameter hybrid functional[14] and Lee-Yang-Parr's gradient corrected correlation functional[15] (B3LYP). The LanL2DZ basis set and effective core potential are used for the Rh atom, and the split-valence 6-31G** basis set is applied for all other atoms. Geometries of the complexes are optimized in the gas phase without any constrains, and the nature of all stationary points is confirmed by normal-mode analysis. Thermal correction based on harmonic frequencies and Gibbs free energy calculations are performed at 298.15 K and 1 atm. The nature of transition states (TSs) is confirmed by performing harmonic vibrational frequencies calculations and normal-mode analyses, which give for each of the TSs herein presented a single imaginary frequency value.

III. RESULTS AND DISCUSSION

Parahydrogenated maleic acid obtained from ADC shows a polarized emission signals at 6.5 ppm in acetone and methanol (Figure 2). Signal enhancement, i.e., the intensity of the polarized emission signal of the formed maleic acid in respect to thermal equilibrium, is about 34 ± 10 (methanol) and 13 ± 5 (acetone). Note that the different signal intensity observed in Figure 2 is not due to hydrogenation yield but must be ascribed to a solvent effect. In fact, as can be derived from the thermal equilibrium spectra (supplementary material),[19] hydrogenation yield is about 30% in acetone and 20% in methanol.

The formation of hyperpolarized longitudinal magnetization derived from parahydrogen on magnetically equivalent protons was already observed[11] and it was demonstrated to be dependent on the intensity of the magnetic field at which the hydrogenation reaction takes place. In that case nuclear relaxation interference mechanism due to cross-correlation between dipolar interaction and chemical shift anisotropy was the reason for the observed hyperpolarized longitudinal magnetization derived from parahydrogen spin order on the A_2 spin system. To get more insights into the formation of the polarized negative signal of maleate, parahydrogenation of ADC is carried out inside the spectrometer by bubbling parahydrogen through the hydrogenation mixture. From comparison of the ^{1}H spectrum acquired using the PASADENA[5] procedure with the experiment carried out in the spectrometer fringe field, it has been found that the intensity of the polarized emission signals is almost the same in these two experiments (Figure 3). PASADENA experiments often require $\pi/4$ pulse to maximize the signal, while in our experiments a $\pi/2$ pulse is used with both experimental methods. The application of a $\pi/4$ pulse is necessary when hyperpolarized spin order $I_z^{H_A} I_z^{H_X}$ must be observed. This hyperpolarized magnetization mode is achieved when the two parahydrogen protons are transferred to chemically different positions, while in the present case they are added to chemically equivalent sites. In the present case, only hyperpolarized longitudinal magnetization can be obtained, than the same pulse angle must be applied to both experiments.

Since polarization is the same when the reaction is carried out inside and outside the spectrometer, it cannot be attributed to magnetic field dependent effects such as frequency

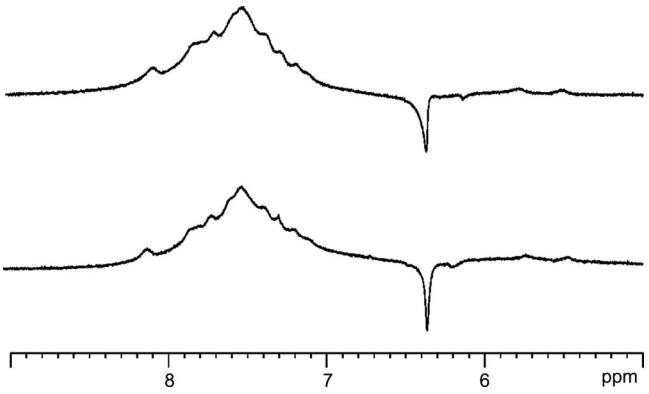

FIG. 3. ^{1}H-NMR spectra obtained from parahydrogenation of natural abundant ^{13}C ADC in acetone carried out by bubbling parahydrogen through the reaction mixture out of the NMR spectrometer (upper spectrum) and inside the magnet (lower spectrum). The broad signal centered at 7.5 ppm is due to catalyst aromatic protons.

difference between the two parahydrogen protons on reaction intermediate as reported by Bargon *et al.*[16] or to chemical shift anisotropy relaxation mechanism. Therefore a different process from that previously reported must be involved.

The presence of ^{13}C nuclei at natural abundance in the substrate also affects hyperpolarization effects in the proton spectrum of the products. In order to investigate if this is the reason for the observed ^{1}H polarized signal, the parahydrogenation reaction is made on the asymmetrically ^{13}C enriched molecule ADC-1-^{13}C. In this experiment we would expect an increase of the polarized emission signal of two orders of magnitude in respect to that observed with the naturally abundant ^{13}C substrate. On the contrary (Figure 4) the ^{1}H signal of maleic acid is less intense with the ^{13}C enriched substrate, probably due to overlap between the emission signal and the antiphase polarized pattern due to asymmetric coupling of the protons with ^{13}C. This allows to get rid of the hypothesis that magnetic asymmetry due to ^{13}C is responsible for the herein reported polarization.

In order to account for the observed hyperpolarized ^{1}H signal on maleate and for the effect of solvent on signal

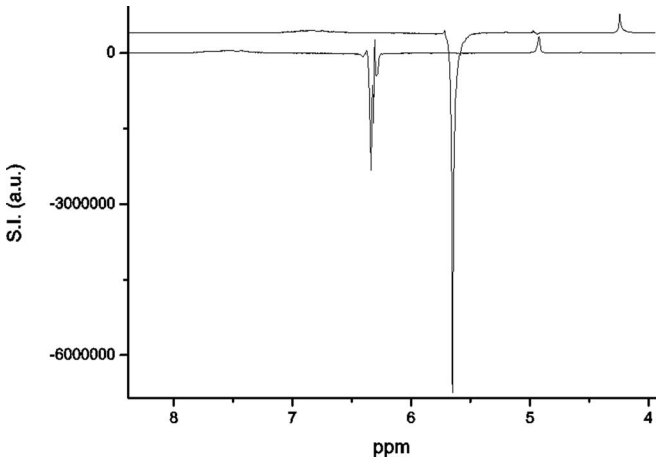

FIG. 4. ^{1}H-NMR polarized olefinic signal of parahydrogenated maleate obtained in methanol: upper spectrum: naturally abundant ^{13}C substrate; lower spectrum: asymmetrically ^{13}C enriched substrate 1-^{13}C-ADC.

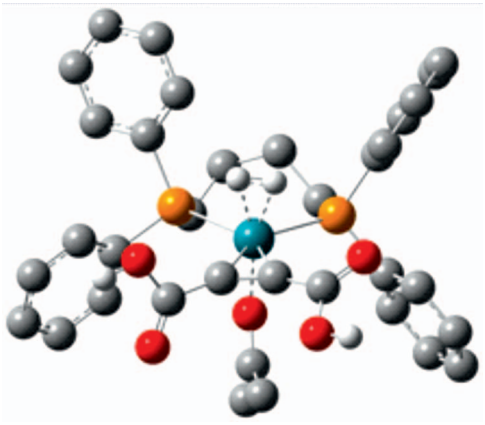

FIG. 5. Optimized structure of the η^2-H_2 rhodium complex (**3'**), using acetone as solvent (for clarity only selected hydrogen atoms are shown).

enhancement, the hydrogenation pathway has been investigated by means of DFT calculations.

A. DFT calculations

After Kubas reported the first complex containing a side-bound dihydrogen (η^2-H_2) ligand,[17] it became clear that hydrogenation mechanisms could occur via η^2-H_2 intermediates. Landis and co-workers clearly show, computationally, the existence of such η^2-H_2 intermediate in [Rh(DuPHOS)]$^+$ assisted hydrogenation.[18]

For the present study, the structure of the η^2-H_2 complex of [Rh(dppb)]$^+$ with a molecule of acetone coordinated is obtained after DFT geometry optimization (Figure 5), confirming that this is a potential intermediate during the hydrogenation process. The intermediate **3'** has a pentacoordinated trigonal bipyramidal molecular geometry, similar to that previously reported for [Rh(DuPHOS)]$^+$.[18] The nature of the stationary point of **3'** was confirmed by normal-mode analysis (the prime $'$ indicates the difference of this intermediate from that reported in Figure 1).

Coordination of acetylene dicarboxylic acid to the metal could potentially occur via several slightly different structures of **3'**, depending on the orientation of carboxylic groups. At least three derivatives differing for the orientation of the HO–OH, HO–O, and O–O moieties of the two COOH groups in respect to the η^2-H_2 ligand can be sketched (see Figure 6).

However, these structures have negligible energy differences. For example, **3'** (HO–O) is more stable than its conformer **3'** (O–O) by 2.2 kJ/mol. Interconversion among conformers occurs by free rotation around the C–COOH bonds.

Starting from the DFT optimized structure **3'**, we search for the transition state (TS) of a reaction in which **3'** could play the role of being either a reagent or a product. The optimized TS structure **3'^{TS}** is only 4.0 kJ/mol higher in energy than **3'** and it has only one imaginary frequency at 642i cm^{-1}. Its vibrational mode is associated with the reaction coordinate that involves motion of the H_2 hydrogen atoms towards breaking the H–H bond and the formation of Rh–H and C–H bonds.

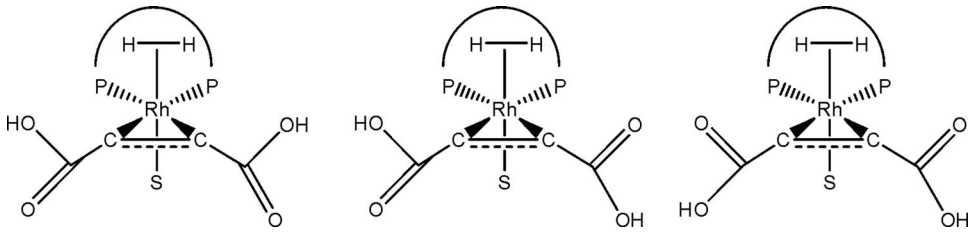

FIG. 6. From left to right HO–OH, HO–O, and O–O conformers of 3 (S = solvent, P∩P = dppb).

It is interesting to note that the calculated rotational barrier of the η^2-H_2 around Rh bond in **3'** is 16.2 kJ/mol,[20] which is higher than that of **3'^{TS}**. Therefore, it is expected that **3'** immediately evolves towards **3'^{TS}**.

The intrinsic reaction coordinate method (IRC), as implemented in Gaussian 09, demonstrated that the structure **3'** is connected to the transition state **3'^{TS}**, i.e., **3'** is either a reagent or a product in a reaction that involves **3'^{TS}**. While the reagent **3'** is close both in energy and shape to **3'^{TS}**, the reaction pathway leading to the product **4'** is energetically steep. In fact, after forty forward IRC points from **3'^{TS}** towards the product, we observe the migration of a H atom with the formation of a C–H bond that lays in the Rh equatorial plane (Figure 7, left). Subsequent full geometry optimization of this structure leads to the product **4'** (Figure 7, right), in which H has been transferred to a carbon atom. The intermediate **4'** is 148.1 kJ/mol lower in energy than **3'**. The newly formed C–H bond lays in the plane of the Rh centre and leads to an agostic Rh···H–C in plane interaction (2.69 Å), which allows Rh to keep a pseudo octahedral coordination mode.

The nearest hydrogen atoms to the hydride hydrogen in **4'** are those of two ortho H phenyls, at a distance of 2.203 and 2.352 Å, respectively. The third phenyl H (down left in Figure 7 right) is at 3.315 Å. On the other hand, the H just transferred to C in **4'**, does not have other Hs in the close proximity, since the nearest H is the hydride at 3.186 Å. These distances are important for the evolution of the polarized NMR signals after parahydrogenation (see Sec. III B).

On the basis of the proposed pathway, the octahedral dihydride complex is never obtained as intermediate, because the η^2-H_2 derivative undergoes a very fast hydrogen transfer to the unsaturated substrate, with a very low activation energy (only 4.0 kJ/mol).

Starting from the monohydride specie **4'**, we search for a TS accounting for the second hydrogen transfer from the metal to the substrate. Figure 8 (left) shows the new TS **4'^{TS}** obtained from **4'**, which is 40.3 kJ/mol higher in energy than **4'**. It has only one imaginary frequency at 847i cm^{-1}, and its vibrational mode is associated with the reaction coordinate involving the motion of H atom along the Rh–C bond. After 40 forward IRC points from **4'^{TS}** we observe the migration of the hydride H atom towards the substrate; subsequent geometry optimization leads to a stable structure **5** (Figure 8, right) in which the alkene is coordinated to Rh, and the solvent is moved away from the metal.

The overall energy diagram is reported in Figure 9, and explains very well the hydrogenation mechanism (Figure 10), including the observed selective *cis* hydrogenation. It is worth to outline that the hydrogenation pathway differs from that proposed in Figure 1, in particular the dihydride intermediate (**3**) is not obtained and the hydrogen molecule evolves directly from the η^2 coordination to intermediate **4'**. Furthermore it must be noticed that, on intermediate **4'**, the proton transferred to carbon is agostic position.

Next, all the above calculations have been repeated using methanol instead of acetone. The obtained results are similar, with lower values of activation energies. **3''^{TS}** (imaginary frequency at 639i cm^{-1}) is only 1.4 kJ/mol higher in energy than **3''** (where the '' specifies methanol instead of acetone), **4''** is 153.8 kJ/mol more stable than **3''**, and **4''^{TS}** (799i cm^{-1}) is now only 19.8 kJ/mol higher than **4''**. These findings point out that the hydrogenation is faster in methanol than in

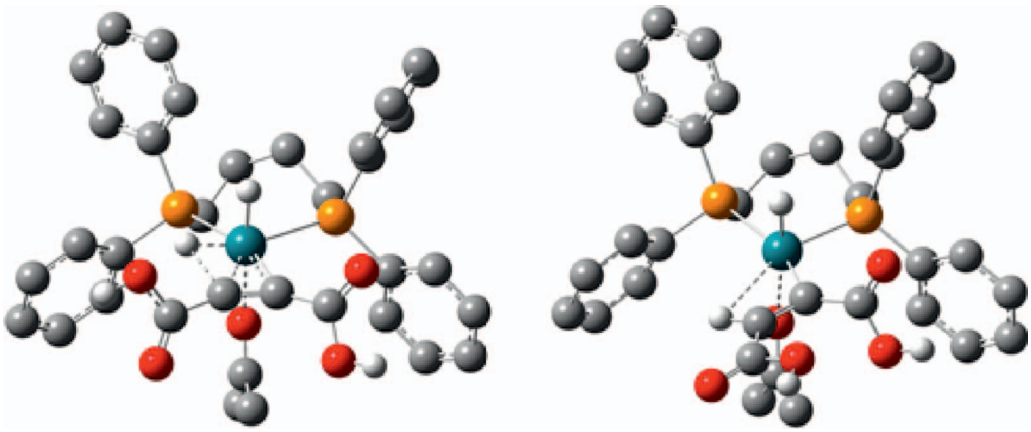

FIG. 7. Structure after 40 IRC iterations (left) and the optimized product **4'** (right).

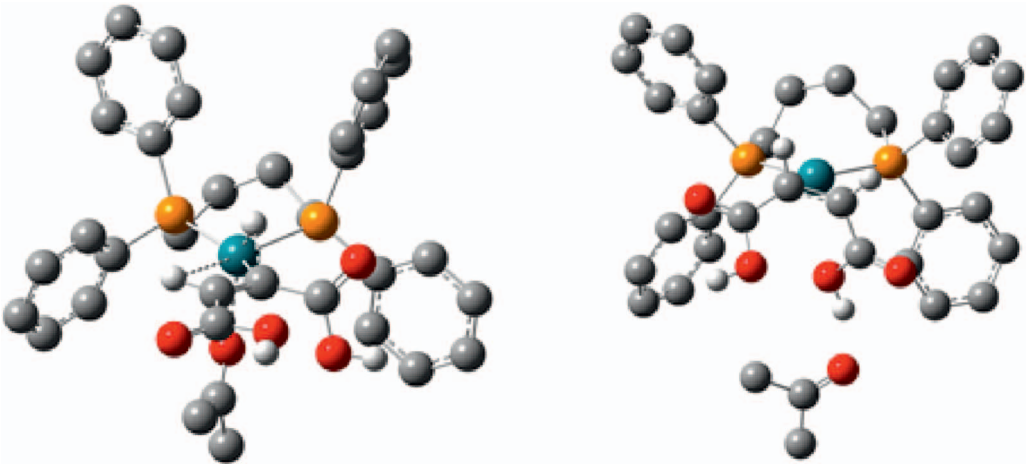

FIG. 8. Transition State **4'**^{TS} obtained using **4'** as starting molecule (left) and optimized structure after hydrogen transfer of the alkene product **5**, still coordinated to Rh.

acetone (the highest energy barrier of the TSs is 40.3 kJ/mol in acetone and 19.8 in methanol) (Table I).

The last step of the mechanism is the release of the hydrogenated alkene. In the case of methanol the structure shown in Figure 10 represents one of the possible steps that close the catalytic cycle, restoring the initial $[Rh(dppb)S_2]^+$ catalyst. It is interesting to note that in MeOH the metal roughly retains its square planar structure, and the two in plane coordination positions are now occupied by two oxygens. The first (on the left of Rh in Figure 11) belongs to the solvent MeOH, and the second is the C–OH oxygen of the hydrogenated acid. It is noteworthy how the hydrogen bond between MeOH and the carboxylic group assists the stabilization of this 9 members ring.

B. Parahydrogen induced polarization

As already mentioned, hyperpolarized longitudinal magnetization (I_z^A) can be obtained from parahydrogen on A_2 spin systems providing that cross-correlation between different relaxation processes of the two parahydrogen protons occurs at an intermediate stage of the reaction.[11,20] Note that cross correlation can be obtained between csa and dipole-dipole interaction but also between two different dipole-dipole relaxation processes that occur at each proton site.

Relaxation of singlet states have been treated into details by Carravetta *et al.*;[21] however, singlet relaxation due to external random fields cannot lead to the formation of longitudinal magnetization, but asymmetric relaxation must occur on species at which the two protons are magnetically (or chemically) different.

On intermediate **4'** the two parahydrogen protons are chemically different and a large frequency shift can be achieved inside the spectrometer magnetic field. However, as the polarized emission signal is the same when the reaction is carried out at low field, asymmetry has to be due to other mechanisms. Asymmetrical coupling of the two protons with heteronuclei of the complex also occurs at this intermediate stage. In particular, coupling with the two ^{31}P nuclei and with ^{103}Rh must be considered, an AA'XX'Y spin system is

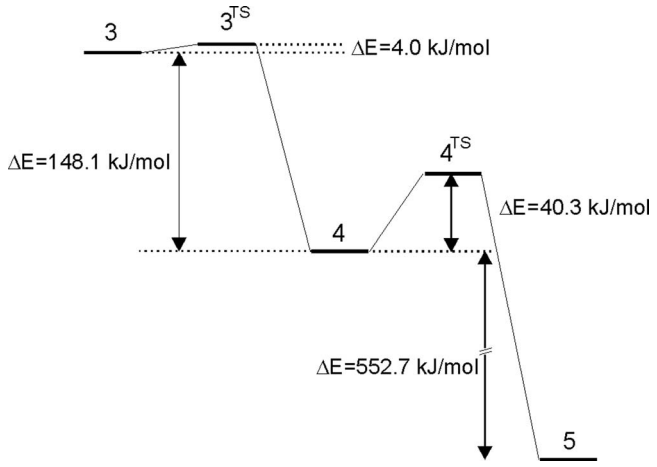

FIG. 9. Schematic representation of the computational results using acetone as solvent.

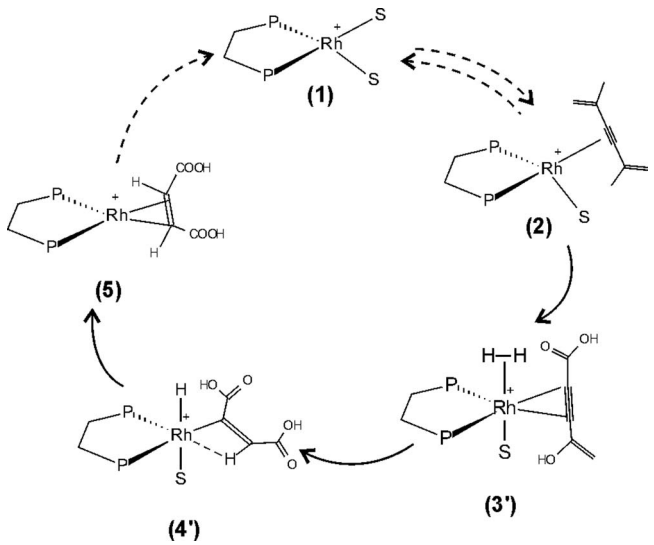

FIG. 10. Hydrogenation pathway obtained for ADC hydrogenation in acetone (S = acetone). The dotted arrows indicate passages to which DFT calculations have not been applied.

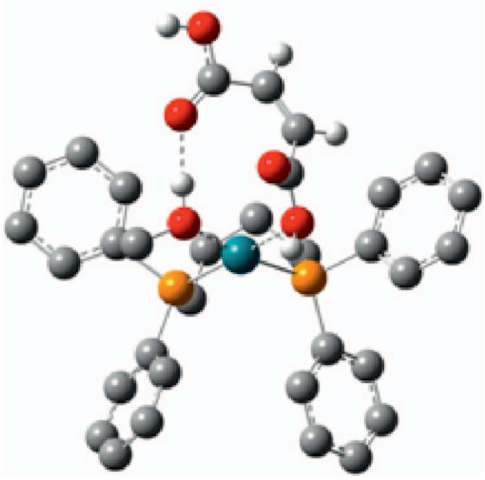

FIG. 11. One of the possible intermediates during the release of the hydrogenated alkene.

formed and mixing of singlet ($|S = (|\alpha\beta - |\beta\alpha)/\sqrt{2}$) and triplet ($|T_0 = (|\alpha\beta + |\beta\alpha)/\sqrt{2}$) states occurs. The states $S'_0 = (c_{21}(t)\, S_0 + c_{22}(t)\, T_0)$ and $T'_0 = (c_{11}(t)\, S_0 + c_{12}(t)\, T_0)$ are formed (the heteroatoms are omitted for simplicity), note that the coefficients are time-dependent and population of the singlet state oscillates between the state S_0' and T_0' as a function of the coefficients (c_{21}) and (c_{11}).

Due to the complexity of the AA'XX'Y spin system, a density matrix approach has been applied to evaluate time evolution of the spin states population using a numerical method.[19] Parahydrogen density operator $\sigma_{S_0} = \frac{1}{4}\mathbf{1} - (I_z^A I_z^{A'} + I_x^A I_x^{A'} + I_y^A I_y^{A'})$ evolves on intermediate **4'**, according to the Liouville-Von Neumann equation, under the action of the J-coupling Hamiltonian,

$$H_J = J_{AA'} \boldsymbol{I}^A \boldsymbol{I}^{A'} + J_{AX} I_z^A I_z^X + J_{AX} I_z^A I_z^{X'} + J_{AX} I_z^{A'} I_z^X + J_{AX} I_z^{A'} I_z^{X'} + J_{AY} I_z^A I_z^Y + J_{A'Y} I_z^{A'} I_z^Y,$$

where A and A' are the agostic and hydride proton respectively, X and X' are the ^{31}P nuclei and Y is ^{103}Rh.

TABLE I. Calculated relative energies (kJ/mol) for intermediates **4'** and **5** and activation barriers for the first (ΔE_1) and second (ΔE_2) hydrogen transfer to the substrate.

	3'^{TS}	**4'**	**4'^{TS}**	**5**	ΔE_1	ΔE_2
Acetone	4.0	−148.1	−108.1	−700.8	4.0	40.3
Methanol	1.4	−153.8	−134.0	−244.9	1.4	19.8

Time dependent population of the spin states S_0' and T_0' are calculated[19] and are represented in Figure 12. Para-hydrogen population oscillates between T_0' and S' states and hyperpolarized longitudinal magnetization is not obtained.

Then we have considered the different dipolar interactions that the two protons experience on intermediate **4'**. As reported in the DFT section, the hydride has two phenyl protons in close proximity while, for the agostic hydrogen, the nearest proton is the hydride, therefore asymmetrical relaxation of the two parahydrogen nuclei on intermediate **4'** occurs.

The single quantum transition probability at each proton is given by $W_1 = (3/20)b^2 J(\omega_1)$,[22] where $b = -(\mu_0/4\pi)(\hbar\gamma^2/r^3)$ and r is the distance between interacting spins, since A is the agostic and A' the hydride proton. It can be obtained that

$$W_1^{A'} = b_{AA'}^2 J(\omega_1) + b_{A-ext}^2 J(\omega_1), \quad (1)$$

$$W_1^{A} = b_{AA'}^2 J(\omega_1), \quad (2)$$

where $b_{AA'}$ is the contribution due to dipolar interaction among the two parahdyrogen protons and $b_{A\text{-}ext}$ is given by dipolar interaction between the hydride proton (A) and the phenyl protons on intermediate **4'**.

Since the singlet and triplet characters of the S_0' and T_0' states oscillate during time, single quantum transition probabilities from the S'_0 states to the states T_- and T_+ are time

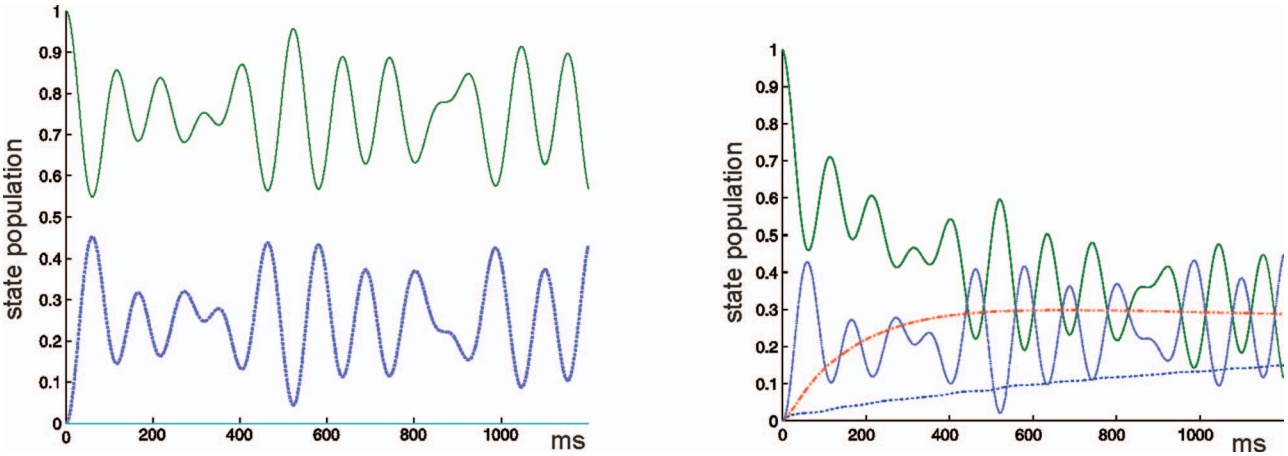

FIG. 12. Time behavior of the spin states populations: (S' (green, continuous line), T' (light blue, small dots line), T_+ (blue, dotted line), and T_- (red, line-dots) calculated on intermediate **4'**, where the AA'XX'Y spin system is formed (AA' are the agostic and hydride proton respectively, X and X' are the ^{31}P nuclei and Y is Rh). Left: without relaxation; right: asymmetrical relaxation on **4'** is considered. ($\tau_c = 2 \times 10^{-10}$ s).

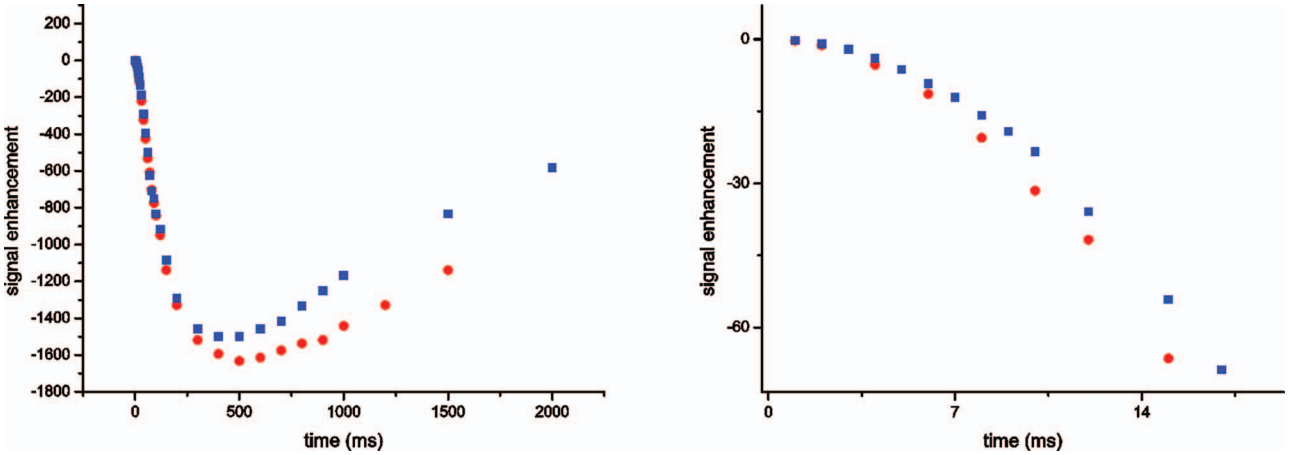

FIG. 13. Intensity of the polarized emission signal as a function of intermediate **4'** lifetime for two different J coupling sets: $J_{AA'} = -3.4$; J_{AX}, $J_{AX'} = 5.8$, 34 Hz; $J_{AY} = 13.4$ Hz; $J_{A'X}$, $J_{A'X'} = 10.8$, 23.8 Hz; $J_{A'Y} = 11$ Hz : blue squares; $J_{AA'} = -1$; J_{AX}, $J_{AX'} = 1$, 17.5 Hz; $J_{AY} = 1$ Hz; $J_{A'X}$, $J_{A'X'} = 11.8$, 24 Hz; $J_{A'Y} = 11$ Hz : red dots.

dependent. They are given by Equations (3)–(6),

$$W_1^{S'-T_-} = \left|\langle T_-|\hat{I}_+^A|S_0'\rangle\right|^2 * W_1^A + \left|\langle T_-|\hat{I}_+^{A'}|S_0'\rangle\right|^2 * W_1^{A'}$$
$$= (c_{21}(t) - c_{22}(t))^2 * W_1^A + (c_{21}(t) + c_{22}(t))^2 * W_1^{A'}, \quad (3)$$

$$W_1^{T_0-T_-} = \left|\langle T_-|\hat{I}_+^A|T_0'\rangle\right|^2 * W_1^A + \left|\langle T_-|\hat{I}_+^{A'}|T_0'\rangle\right|^2 * W_1^{A'}$$
$$= (c_{11}(t) - c_{12}(t))^2 * W_1^A + (c_{11}(t) + c_{12}(t))^2 * W_1^{A'}, \quad (4)$$

$$W_1^{S'-T_+} = \left|\langle T_+|\hat{I}_-^A|S_0'\rangle\right|^2 * W_1^A + \left|\langle T_+|\hat{I}_-^{A'}|S_0'\rangle\right|^2 * W_1^{A'}$$
$$= (c_{21}(t) + c_{22}(t))^2 * W_1^A + (c_{21}(t) - c_{22}(t))^2 * W_1^{A'}, \quad (5)$$

$$W_1^{T_0-T_+} = \left|\langle T_+|\hat{I}_-^A|T_0'\rangle\right|^2 * W_1^A + \left|\langle T_+|\hat{I}_-^{A'}|T_0'\rangle\right|^2 * W_1^{A'}$$
$$= (c_{11}(t) + c_{12}(t))^2 * W_1^A + (c_{11}(t) - c_{12}(t))^2 * W_1^{A'}. \quad (6)$$

Note that W_1 (S' − T_-) ≠ W_1 (S' − T_+) and W_1 (T_0 − T_-) ≠ W_1 (T_0 − T_+) then the states T_+ and T_- become asymmetrically populated and longitudinal magnetization is obtained on the product. Time behaviour of spin states populations due to asymmetric relaxation on intermediate 4' has been numerically calculated and is graphically reported in Figure 12. The J coupling values are those reported in Ref. 10 for similar compounds and $\tau_c = 2 \times 10^{-10}$ s has been obtained from T_1 measurement of the olefinic protons of cyclooctane coordinated to Rh in the [Rh(COD) dppb] complex.[23]

Signal enhancement (S.E.) referred to the thermally polarized signal, derives from the population difference between the states T_- and T_+ and its maximum would be achieved if only one spin level (T_+ or T_-) became populated. In that case, it would be given by the inverse of the thermal equilibrium signal for protons $\frac{\gamma_H \hbar B_0}{2kT}$, i.e., 20 400 times, but, as parahydrogen enrichment is 52%, maximum polarization would be only 6800. Starting from the population difference between T_- and T_+ we obtain that the maximum intensity of the polarized emission signal, reached at about 400–500 ms lifetime, would be 1500–1600 times in respect to the equilibrium signal. At that time, the spin states populations are $P_{T-} = 0.29$ and $P_{T+} = 0.07$ for **a** (signal enhancement would be 1500 times) and $P_{T-} = 0.3$ and $P_{T+} = 0.06$ for **b** (S.E. 1600). Time behavior of the polarized signal intensity as a function of intermediate **4'** lifetime is reported in Figure 13.

As far as the experimental results are concerned, signal enhancement for the olefinic signal of maleic acid is about 35 times in methanol. Note that the reaction, from the shaking of the NMR tube to spectrum acquisition, spans about 10" time. Assuming that the amount of polarized product is constant during that time and since T_1 of the polarized signal is about 7 s (measurement carried out at 14.1T using the inversion recovery sequence) we have calculated[19] that signal enhancement at time zero, i.e., immediately after the product formation, is about 60 times. This signal enhancement is achieved when intermediate **4'** lifetime is between 14 and 16 ms (Figure 13). These values are not too far from that experimentally measured by Halpern *et al.* using a kinetic approach (5.9 ms)[24] on the olefinic substrate MAC (methyl (Z)-a-acetamidocinnamate). Higher intermediate stability might be due to the fact that, in our case, triple bond is hydrogenated instead of double, furthermore, J coupling values used in our calculations are not referred to the herein reported substrate.

IV. CONCLUSIONS

The combined study carried out with DFT calculation and PHIP clarifies the hydrogenation mechanism of ADC carried out by the a Rh(I) complex containing a chelating phosphine as ligand.

By means of DFT calculations, intermediate structures and their relative stability have been found in two different solvents, acetone and methanol. The hydrogenation pathway thus obtained slightly differs from that previously reported,[1]

in which a dihydride intermediate was formed, because the η^2 coordination of the hydrogen molecule evolves with a very low activation barrier to the transfer of one proton to the substrate to yield an agostic and a hydride moiety, respectively (**4'**).

This short-lived intermediate plays an important role in determining hyperpolarization effects on the product. It is demonstrated that the hyperpolarized emission signal observed in the ^{1}H-NMR spectrum on maleic acid derives from asymmetric relaxation of the two parahydrogen protons while they form an AA'XX'Y spin system with the ^{31}P and ^{103}Rh nuclei of the catalyst. The intensity of this signal depends on the intermediate lifetime, on dipolar interactions of the two parahydrogen nuclei with neighboring protons and on their J coupling with all the heteronuclei of the catalyst. From the experimentally observed signal enhancement and on the basis of ^{1}H-^{1}H distances obtained from DFT calculated structure it is possible to estimate the intermediate lifetime.

We should note that on intermediate **5**, where the A_2 spin system is restored, relaxation processes due to external random fields[21] tend to bring population of the singlet state to equilibrium. However, at this stage, polarized longitudinal magnetization cannot be obtained, but population of the triplet states rapidly equilibrate towards equilibrium and the intensity of the emission signal, formed at the previous stage, is diminished.

These can be useful insights for the design of new Rh(I) catalysts endowed with an improved efficiency for parahydrogen hyperpolarization purposes.

AKNOWLEDGMENTS

The authors F. Reineri and S. Aime gratefully acknowledge Piedmont Region (Italy) for financial support (bando POR-FESR 2007, Asse 1, Misura I.1.1).

[1] R. A. Sanchez-Delgado and M. Rosales, Coord. Chem. Rev. **196**, 249 (2000).
[2] I. D. Gridnev and T. Imamoto, Acc. Chem. Res. **37**, 633 (2004).
[3] I. D. Gridnev and T. Imamoto, Chem. Commun. **2009**, 7447.
[4] I. D. Gridnev, T. Imamoto, G. Hoge, M. Kouchi, and H. Takahashi, J. Am. Chem. Soc. **130**, 2560 (2008).
[5] J. Natterer and J. Bargon, Prog. Nucl. Magn. Reson. Spectrosc. **31**, 293 (1997).
[6] S. B. Duckett and C. J. Sleigh, Prog. Nucl. Magn. Reson. Spectrosc. **34**, 71 (1999).
[7] P. Hübler, R. Giernoth, G. Kümmerle, and J. Bargon, J. Am. Chem. Soc. **121**, 5311 (1999).
[8] P. Kating, A. Wandelt, R. Selke, and J. Bargon, J. Phys. Chem. **97**, 13313 (1993).
[9] R. U. Kirss and R. Eisenberg, J. Organomet. Chem. **359**, C22 (1989).
[10] R. Giernoth, H. Heinrich, N. J. Adams, R. J. Deeth, J. Bargon, and J. M. Brown, J. Am. Chem. Soc. **122**, 12381–12382 (2000).
[11] S. Aime, R. Gobetto, and D. Canet, J. Am. Chem. Soc. **120**, 6770 (1998).
[12] M. B. Franzoni, L. Buljubasich, H. W. Spiess, and K. Munnemann, J. Am. Chem. Soc. **134**, 10393 (2012).
[13] F. Reineri, A. Viale, G. Giovenzana, D. Santelia, W. Dastrù, R. Gobetto, and S. Aime, J. Am Chem. Soc. **130**, 15047 (2008).
[14] A. D. Becke, J. Chem. Phys. **98**, 5648 (1993).
[15] C. Lee, W. Yang, and R. G. Parr, Phys. Rev. B **37**, 785 (1988).
[16] J. Bargon, J. Kandels, and P. Kating, J. Chem. Phys. **98**, 6150 (1993).
[17] G. J. Kubas, R. R. Ryan, B. I. Swanson, P. J. Vergamini, and H. J. Wasserman, J. Am. Chem. Soc. **106**, 451 (1984).
[18] S. Feldgus and C. R. Landis, J. Am. Chem. Soc. **122**, 12714 (2000).
[19] See supplementary material at http://dx.doi.org/10.1063/1.4867269 for graphic of calculated rotational barrier of hydrogen on intermediate **3**, Matlab function used to calculate time dependent density operator and spin states populations on intermediate **4'**, extrapolation of the experimental signal enhancement at time zero, and ^{1}H-NMR spectra acquired after the thermal equilibrium of the polarized spectra reported in Figure 2 has been restored.
[20] D. Canet, Prog. Nucl. Magn. Reson. Spectrosc. **21**, 237 (1989).
[21] M. Carravetta and M. H. Levitt, J. Chem. Phys. **122**, 214505 (2005).
[22] M. H. Levitt, *Spin Dynamics* (John Wiley & Sons, Chichester, 2001), p. 529.
[23] Olefinic protons of cyclooctadiene coordinated to Rh in the complex [RhCODdppb], acetone, RT, 600 MHz, $T_1 = 1.15$ s.
[24] A. S. C. Chan and J. Halpern, J. Am. Chem. Soc. **102**, 838 (1980)